
OPPO: Bayesian Value Recursion for Token-Level Credit Assignment in LLM Reasoning

Yu Li¹ Rui Miao² Tian Lan¹ Zhengling Qi¹

¹George Washington University ²The University of Texas at Dallas

Abstract

Reinforcement learning with verifiable rewards has become the standard recipe for improving LLM reasoning, but the dominant algorithm GRPO assigns a single trajectory-level advantage to every token, diluting the signal at pivotal reasoning steps and injecting noise at uninformative ones. Critic-free alternatives derived from on-policy distillation supply per-token signals through oracle-conditioned likelihood ratios, yet apply each signal in isolation from the trajectory-level evidence accumulated up to that position. We propose Oracle-Prompted Policy Optimization (OPPO), which rests on a single observation: the oracle signal used by prior distillation-style methods for local discrimination is also the natural Bayesian update of the model’s belief about eventual success. Accumulating the signal along a trajectory yields, in closed form and at the cost of one extra forward pass, a running estimate of the success probability at every position, together with a token-level advantage that requires no learned value network and no additional rollouts. A first-order analysis factorizes the advantage into the per-token discrimination signal used by distillation methods modulated by a state weight that concentrates credit on genuinely pivotal tokens, with a directional variance-reduction guarantee. The framework admits two estimators differing only in which model scores the evidence: a *self-oracle* that reuses the student and recovers the on-policy distillation reward as a strict special case, and a *teacher-oracle* that delegates scoring to a stronger frozen model. On two base LLMs across seven mathematics, science, and code reasoning benchmarks, OPPO improves over GRPO, DAPO, and SDPO by up to +6.0 points on AMC’23 and +5.2 points on AIME’24, with gains that widen monotonically with response length.

1 Introduction

Reinforcement learning with verifiable rewards (RLVR) has become a central paradigm for improving the reasoning capabilities of large language models [9, 34, 13]. In the standard pipeline, a model generates a complete reasoning trajectory, receives a binary reward based on the correctness of the final answer, and updates its policy to increase the likelihood of generating correct trajectories. Group Relative Policy Optimization (GRPO) [9] is the most widely adopted on-policy algorithm in the paradigm, estimating the advantage of each trajectory relative to a group of sampled responses and feeding the signal into a clipped policy gradient update.

GRPO broadcasts a single scalar advantage to every token position [24]. In a reasoning chain of several hundred tokens, only a small subset of tokens typically determine the outcome, namely those corresponding to a strategy selection, a key algebraic step, or a critical logical deduction [27, 32]. By assigning equal credit to every position, GRPO dilutes the learning signal at pivotal tokens and injects noise through undeserved gradient updates at uninformative ones, and the problem worsens as reasoning chains grow longer [36, 16].

Recent work has pursued two strategies. The first refines the GRPO framework while retaining the trajectory-level advantage. Dr.GRPO [24], DAPO [36], GSPO [39], and GMPO [38] modify

the importance ratio, clipping, or advantage normalization, yet every token still receives the same advantage [10]. The second seeks finer-grained credit at the token level. Monte Carlo resampling methods such as VinePPO [19] and TreeRL [11] require orders of magnitude more inference, implicit process reward models such as PRIME [6] require online updating, and segment-level aggregation in SPO [10] pools descendant outcomes within shared prefixes. Most relevant to the present work, on-policy distillation methods with privileged information [2, 8, 25, 35, 12] condition the model on the ground-truth answer y^* and use the resulting log-likelihood ratio $\log \lambda_t = \log \pi_{\text{teacher}}(y_t | s_t) - \log \pi_{\text{student}}(y_t | s_t)$ as a token-level credit signal, where $\log \lambda_t$ is the one-step expert log-ratio between the success-conditional optimal policy π^* and the student. Every such method, however, applies $\log \lambda_t$ with uniform weight across positions and treats each token’s credit as an isolated one-step quantity decoupled from the cumulative evidence along $y_{<t}$.

Motivated by this gap, we propose Oracle-Prompted Policy Optimization (OPPO), which rests on a single observation: the per-token oracle signal used in distillation-style methods is also the natural Bayesian update of the model’s belief about eventual success. Accumulating the signal along a trajectory yields, in closed form and at no extra rollout cost, a running estimate of the success probability at every position, and from it a token-level advantage that requires no learned value network and sums exactly to the trajectory’s outcome relative to its prior. The recursion admits two estimators that differ only in which model scores the evidence: a self-oracle reuses the student in one extra forward pass and recovers the on-policy distillation reward as a strict special case, while a teacher-oracle delegates scoring to a stronger frozen model. The advantage factorizes as the per-token discrimination signal modulated by a state weight $V_t(1 - V_t)$ that peaks where the running belief is most uncertain and vanishes once the trajectory has committed, concentrating credit on pivotal tokens without any tunable hyperparameter. A direction-anchoring step ties the sign of each token-level advantage to the sequence-level outcome, preserving the verifier as the sole arbiter of which trajectories are reinforced while letting the Bayesian machinery redistribute credit within each trajectory.

Our contributions are as follows.

- Showing that the OPD per-token reward $\log \lambda_t$ is simultaneously an expert log-ratio surrogate for A_t^* and the Bayesian sufficient statistic for V_t , with the choice of probability measure cleanly selecting the self-oracle or teacher-oracle estimator.
- Deriving a closed-form Bayesian value recursion that produces a token-level advantage with no learned critic and no extra rollouts, satisfies the telescoping budget $\sum_t A_t = R - V_0$, and admits the factorization $A_t \approx V_t(1 - V_t) \log \lambda_t$ with a directional variance-reduction guarantee.
- Integrating the recursion into the GRPO pipeline via direction anchoring and evidence clipping at the cost of one extra forward pass per trajectory, with identical downstream computation under either oracle.
- Evaluating the method on Qwen3 and Phi reasoning models across seven reasoning benchmarks, where the proposed framework consistently surpasses representative trajectory-level and oracle-conditioned baselines, with up to +5.7 points on AMC’23 and +5.2 points on AIME’24 under Teacher-OPPO on DAPO and gains that widen monotonically with response length.

2 Preliminaries

2.1 Reinforcement Learning for LLM Reasoning

We model autoregressive LLM generation as a finite-horizon Markov decision process $(\mathcal{S}, \mathcal{V}, \pi_\theta, R)$ over a finite vocabulary \mathcal{V} . Given a query x , the state at step t is the prefix $s_t \triangleq (x, y_{<t})$ with $y_{<t} \triangleq (y_1, \dots, y_{t-1})$ and $s_1 = (x)$. The policy $\pi_\theta(\cdot | s_t) \in \Delta(\mathcal{V})$ samples a token y_t , yielding the deterministic transition $s_{t+1} = (s_t, y_t)$. Generation terminates at the first step $T \leq T_{\max}$ where y_T is the end-of-sequence symbol. A verifier assigns a terminal binary reward $R(\tau) \in \{0, 1\}$ indicating answer correctness, with all intermediate rewards equal to zero. Training maximizes the expected return through policy gradient

$$J(\theta) \triangleq \mathbb{E}_{x \sim \mathcal{D}, \tau \sim \pi_\theta(\cdot | x)}[R(\tau)], \quad \nabla_\theta J(\theta) = \mathbb{E} \left[\sum_{t=1}^T A_t(s_t, y_t) \nabla_\theta \log \pi_\theta(y_t | s_t) \right], \quad (1)$$

where \mathcal{D} is the query distribution and $A_t : \mathcal{S} \times \mathcal{V} \rightarrow \mathbb{R}$ is any per-token advantage estimator unbiased against $Q_t(s_t, y_t) \triangleq \mathbb{E}_{\pi_\theta} [R \mid s_t, y_t]$ when paired with the score function $\nabla_\theta \log \pi_\theta(y_t \mid s_t)$.

GRPO [9] forgoes a learned value baseline by drawing a group of $G \geq 2$ trajectories $\{\tau_i\}_{i=1}^G \sim \pi_\theta(\cdot \mid x)$ per query and assigning every token in τ_i the trajectory-level standardized advantage

$$\hat{A}_i^{\text{GRPO}} \triangleq \frac{R_i - \mu}{\sigma + \varepsilon}, \quad \mu \triangleq \frac{1}{G} \sum_{j=1}^G R_j, \quad \sigma \triangleq \sqrt{\frac{1}{G} \sum_{j=1}^G (R_j - \mu)^2}, \quad (2)$$

so that $A_t(\tau_i) \equiv \hat{A}_i^{\text{GRPO}}$ for all $t \in \{1, \dots, T_i\}$. The estimator is exchangeable in t , so if a subset $\mathcal{C}(\tau)$ of cardinality $k \ll T$ carries the causal responsibility for R , the signal at $t \in \mathcal{C}(\tau)$ is attenuated by a factor of k/T while the remaining $T - k$ positions receive gradient mass with zero expected contribution [14, 21].

The cleanest reference quantity for token-level credit is the on-policy state value

$$V_t \triangleq P^{\pi_\theta}(R = 1 \mid x, y_{1:t-1}), \quad V_0 \triangleq P^{\pi_\theta}(R=1 \mid x), \quad V_{T+1} \triangleq R, \quad (3)$$

which satisfies the Bellman consistency $V_t = \mathbb{E}_{y_t \sim \pi_\theta} [V_{t+1}]$. The ideal token-level advantage is the one-step temporal difference $A_t \triangleq V_{t+1} - V_t = Q_t(s_t, y_t) - V_t(s_t)$, and telescoping along the trajectory gives

$$\sum_{t=1}^T A_t = V_{T+1} - V_0 = R - V_0, \quad (4)$$

so the question is how to distribute the credit budget $R - V_0$ across the T positions. PPO [29] trains a value network $V_\phi(s_t)$ to approximate Eq. (3) at substantial memory cost; GRPO sets $V_t \equiv V_0$ and distributes $R - V_0$ uniformly. Note that token-level estimators concentrate the learning signal on the subset of positions causally responsible for R , while estimators constant in t inject the variance of R uniformly across all positions [23, 31].

2.2 On-Policy Distillation

On-policy distillation (OPD) pairs a student policy π_θ with a frozen teacher π_T and supervises π_θ on its own rollouts under a per-token divergence [2, 8, 25]. In the reasoning setting most relevant to RLVR, the teacher is conditioned on privileged information such as the ground-truth answer y^* , so that $\pi_T(\cdot \mid x, y_{<t}) \equiv \pi_T(\cdot \mid x, y^*, y_{<t})$ approximates the success-conditional next-token distribution $P(\cdot \mid x, y_{<t}, R=1)$ [37, 12]. Drawing $y_{1:T} \sim \pi_\theta(\cdot \mid x)$, OPD minimizes the on-policy summed reverse KL

$$\mathcal{L}_{\text{OPD}}(\theta) \triangleq \mathbb{E}_{x, y_{1:T} \sim \pi_\theta(\cdot \mid x)} \left[\sum_{t=1}^T \text{KL}(\pi_\theta(\cdot \mid s_t) \parallel \pi_T(\cdot \mid s_t)) \right]. \quad (5)$$

Standard practice [2, 25] treats the rollout as a stop-gradient sample and differentiates only the inner KL through the student logits, under which the contribution at the sampled token y_t reduces to

$$\nabla_\theta \mathcal{L}_{\text{OPD}}(\theta) \Big|_{y_t} = -\log \lambda_t^{\text{OPD}} \cdot \nabla_\theta \log \pi_\theta(y_t \mid s_t), \quad \log \lambda_t^{\text{OPD}} \triangleq \log \pi_T(y_t \mid s_t) - \log \pi_\theta(y_t \mid s_t). \quad (6)$$

Comparing Eq. (6) with Eq. (1) shows that the OPD update is a REINFORCE estimator in which $\log \lambda_t^{\text{OPD}}$ plays the role of a per-token reward rather than an advantage. The reward coincides with the KL-shaping term in PPO-based RLHF [29] when the privileged teacher serves as the reference policy and the environment reward vanishes, so OPD is the special case of token-level PPO without a learned value baseline and without trust-region clipping. Every position is updated independently of its place in the trajectory, with the local signal $\log \lambda_t^{\text{OPD}}$ decoupled from both the cumulative agreement along $y_{<t}$ and the terminal outcome R [35, 31].

Advantage under the optimal policy. The unbiasedness condition below Eq. (1) leaves freedom in the reference policy under which A_t is defined: replacing $A_t^{\pi_\theta}$ with the advantage under a policy π^* that dominates π_θ in value preserves a valid policy-improvement direction [29, 14]. Let

$$\pi^*(y_t \mid s_t) \triangleq P(y_t \mid x, y_{<t}, R=1), \quad V_t^{\pi^*}(s_t) \triangleq P^{\pi^*}(R=1 \mid s_t), \quad (7)$$

denote the success-conditional optimal policy and its value, with $A_t^{\pi^*} \triangleq Q_t^{\pi^*}(s_t, y_t) - V_t^{\pi^*}(s_t)$ the corresponding one-step advantage. Equation (6) then admits a clean re-reading: the OPD teacher is

an approximation $\pi_T \approx \pi^*$, so $\log \lambda_t^{\text{OPD}}$ is the one-step expert log-ratio between π^* and π_θ , serving as a per-token surrogate for $A_t^{\pi^*}$ in the spirit of advantage-weighted regression.

Bridge to our method. So far we have identified two complementary failure modes of existing methods. The GRPO advantage in Eq. (2) resolves the credit budget $R - V_0$ uniformly across all T tokens, while the OPD signal $\log \lambda_t$ in Eq. (6), an expert log-ratio under π^* , is purely local and ignores both the cumulative evidence along $y_{<t}$ and the terminal outcome R . A principled estimator should sit between the two extremes, retaining OPD’s dense π^* -anchored signal while reweighting it by a position-dependent coefficient that tracks the running posterior of success encoded by Eq. (3), recovering an approximation to $A_t/A_t^{\pi^*}$ without a learned value network.

3 Bayesian Evidence Aggregation

The bridge of Section 2.2 singled out V_t as the right object for token-level credit assignment: the ideal advantage $A_t = V_{t+1} - V_t$ should telescope to $R - V_0$ in Eq. (4), so any accurate tracker of V_t distributes the budget across tokens automatically but the challenge is to track V_t without a learned critic. In this section, we first show that the problem reduces to learning an additive log-odds update driven by a per-token Bayes factor; Then we construct two tractable surrogate for the Bayes factors.

3.1 Bayesian Value Recursion

Applying Bayes’ theorem to update the success probability after observing y_t gives

$$V_{t+1} = P^{\pi_\theta}(R=1 | x, y_{1:t}) = \frac{P(y_t | x, y_{<t}, R=1) V_t}{P(y_t | x, y_{<t})}. \quad (8)$$

Define the per-token Bayes factor between the success and failure branches as

$$\lambda_t^* \triangleq \frac{P(y_t | x, y_{<t}, R=1)}{P(y_t | x, y_{<t}, R=0)} = \frac{P(y_t | x, y_{<t}, y_T=y^*)}{P(y_t | x, y_{<t}, y_T \neq y^*)}, \quad (9)$$

and let $\ell_t \triangleq \log \frac{V_t}{1-V_t}$ collect the running log-odds of success. The probability P in Eqs. (8)–(9) can be taken under either π_θ or π^* from Eq. (7), yielding valid Bayesian recursions for $V_t^{\pi_\theta}$ and $V_t^{\pi^*}$ respectively, with the latter targeted by the expert log-ratio of Section 2.2, though they are not exactly the same. Using the law of total probability $P(y_t | x, y_{<t}) = P(y_t | x, y_{<t}, R=1) V_t + P(y_t | x, y_{<t}, R=0) (1 - V_t)$, Eq. (8) can be rewritten as the additive log-odds recursion

$$V_{t+1} = \frac{\lambda_t^* V_t}{\lambda_t^* V_t + (1 - V_t)}, \quad \ell_{t+1} = \ell_t + \log \lambda_t^*, \quad (10)$$

in which every token contributes additively to ℓ_t via its log-Bayes-factor. Unrolling from $\ell_0 = \text{logit}(V_0)$ and applying the sigmoid yields the closed-form value, the corresponding token-level advantage, and a telescoping credit identity, respectively,

$$V_t = \sigma\left(\ell_0 + \sum_{s<t} \log \lambda_s^*\right), \quad A_t = \sigma(\ell_t + \log \lambda_t^*) - \sigma(\ell_t), \quad (11)$$

$$\sum_{t=1}^T A_t = \sigma(\ell_{T+1}) - \sigma(\ell_0) = R - V_0. \quad (12)$$

Two structural properties follow. Since σ is Lipschitz with constant $\frac{1}{4}$, every token satisfies $|A_t| \leq \frac{1}{4} |\log \lambda_t^*|$, and the universal range bound $|A_t| \leq 1$ applies regardless of $\log \lambda_t^*$, so the per-token contribution is jointly bounded by $\min(\frac{1}{4} |\log \lambda_t^*|, 1)$. Equation (12) fixes the total credit by the outcome and the prior alone, so any estimator that respects the additive log-odds structure of Eq. (10) distributes the GRPO budget across tokens with no further bookkeeping. Token-level credit assignment therefore reduces to estimating $\log \lambda_t^*$, which is defined in terms of the success- and failure-conditional next-token distributions, which are not directly observable.

3.2 Two Oracle Surrogates for Bayesian Evidence

We construct estimators of λ_t^* under either probability measure (π_θ or π^*). Both arise from the same pair of modeling choices applied to whichever scorer $\hat{\pi}$ realizes the measure.

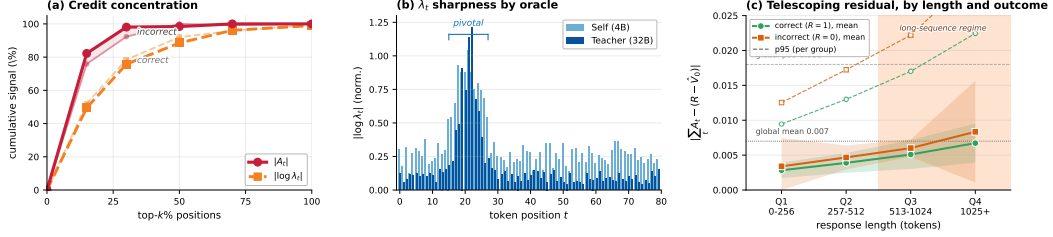


Figure 1: Empirical analysis on 200 MATH-500 trajectories from Qwen3-4B-Instruct. (a) $|A_t|$ concentrates more sharply than $|\log \lambda_t|$, with the gap widest on incorrect trajectories where V_t saturates early. (b) The 32B teacher produces sharper $|\log \lambda_t|$ at pivotal tokens and lower background in determined regions. (c) Telescoping budget residual stratified by length quartile and outcome. Solid lines mark the per-stratum mean of $|\sum_t A_t - (R - \hat{V}_0)|$ with 95% confidence bands. The shaded region marks the long-sequence regime where evidence clipping caps the recursion.

Oracle Conditioning

The success-conditional distribution is approximated by appending y^* to the prompt:

$$P(y_t | x, y_{<t}, R=1) \approx \hat{\pi}(y_t | x, y_{<t}, y^*). \quad (13)$$

The justification is the privileged-teacher rationale of Section 2.2: conditioning on y^* constrains the scorer to tokens consistent with reaching the correct answer.

Failure Branch

The failure-conditional distribution is approximated by the marginal under the same scorer:

$$P(y_t | x, y_{<t}, R=0) \approx \hat{\pi}(y_t | x, y_{<t}). \quad (14)$$

The marginal admits the decomposition $\hat{\pi}(y_t | s_t) = P(y_t | s_t, R=1) V_t + P(y_t | s_t, R=0) (1 - V_t)$: the failure branch dominates as $V_t \rightarrow 0$ and the approximation is tightest where incorrect trajectories spend most of their length, while the gap is largest near $V_t = \frac{1}{2}$ where the state weight $V_t(1 - V_t)$ peaks.

Substituting Modeling Choices 3.2 and 3.2 into Eq. (9) yields the unified estimator

$$\lambda_t \triangleq \frac{\hat{\pi}(y_t | x, y_{<t}, y^*)}{\hat{\pi}(y_t | x, y_{<t})}, \quad \log \lambda_t = \log \hat{\pi}(y_t | x, y_{<t}, y^*) - \log \hat{\pi}(y_t | x, y_{<t}), \quad (15)$$

parameterized by a single scorer $\hat{\pi}$. Setting $\hat{\pi} = \pi_\theta$ yields the *self-oracle*, which requires only one extra forward pass per trajectory and recovers the OPD per-token reward of Eq. (6) exactly, since the OPD privileged teacher is the student conditioned on y^* [37]. Setting $\hat{\pi} = \pi_\phi$ for a frozen scorer that approximates π^* at lower KL distance than π_θ [2, 25] yields the *teacher-oracle*, which reduces approximation error at the cost of a separate scoring model; π_ϕ receives no gradient updates and need not be instruction-tuned, since its role is likelihood scoring rather than generation.

The pointwise gap between either estimator and the exact Bayes factor is captured by the success-branch KL

$$\epsilon_t \triangleq D_{\text{KL}}(P(\cdot | x, y_{<t}, R=1) \parallel \hat{\pi}(\cdot | x, y_{<t}, y^*)), \quad (16)$$

which traces a design axis: the self-oracle yields the largest ϵ_t , and a perfect teacher drives $\epsilon_t \rightarrow 0$, recovering $\lambda_t = \lambda_t^*$ and the exact recursion. Substituting λ_t for λ_t^* in Eq. (10) gives the implementable form, with the budget residual controlled by the cumulative oracle quality $\sum_t \epsilon_t$ (Appendix D.1). The telescoping identity in Eq. (12) applies to the raw advantage before clipping, sign anchoring, and group normalization in Section 4; the implemented training advantage redistributes credit within each trajectory and inherits its direction from the verifier. Figure 1(c) stratifies the residual by length quartile and outcome: the mean rises monotonically from Q1 to Q4 in both classes, with $R=0$ above $R=1$ because V_t saturates earlier on incorrect rollouts.

3.3 Further Discussion and Empirical Validation

Subtracting V_t from both sides of Eq. (10) gives the closed-form identity

$$A_t = \frac{V_t(1 - V_t)(\lambda_t - 1)}{\lambda_t V_t + 1 - V_t}. \quad (17)$$

For $|\lambda_t - 1|$ small, $\lambda_t - 1 \approx \log \lambda_t$ and the denominator approaches 1, yielding the first-order approximation

$$A_t \approx V_t(1 - V_t) \cdot \log \lambda_t. \quad (18)$$

The factorization separates two roles: the oracle evidence $\log \lambda_t$ provides per-token discrimination between success and failure branches, identical to the gradient signal of on-policy distillation in Eq. (6), while the state weight $V_t(1 - V_t)$ modulates the evidence by the running belief. Reliability diagrams in Appendix H.1 confirm that intermediate V_t at $t = T/4, T/2, 3T/4$ is well calibrated.

Two predictions follow. Since $V_t(1 - V_t)$ collapses once the running belief commits, credit concentrates on undetermined positions; on incorrect trajectories V_t saturates toward 0 early, so the state weight collapses even where $\log \lambda_t$ remains elevated by answer-correlated content. Figure 1(a) confirms the prediction: the cumulative signal of $|A_t|$ rises more steeply than that of $|\log \lambda_t|$, with the gap widest on incorrect trajectories. A stronger oracle should additionally sharpen λ_t at pivotal positions while keeping the magnitude small elsewhere, and Figure 1(b) bears this out: the 32B teacher concentrates $|\log \lambda_t|$ more tightly around strategy-selection tokens than the 4B self-oracle. The prior V_0 supplies a complementary adaptation: $V_0(1 - V_0)$ multiplies the entire trajectory, down-weighting easy and unsolvable queries throughout, which yields prompt-difficulty filtering without manual thresholding [6].

The state weight admits a variance-reduction interpretation under an idealized score-vector assumption. Writing the policy gradient as $\hat{g} = \sum_t w_t h_t$ with $h_t = \nabla_\theta \log \pi_\theta(y_t | x, y_{<t})$ and treating the h_t as uncorrelated across positions, the variance gap between the state-blind weighting $w_t = \log \lambda_t$ and the Bayesian weighting $w_t = V_t(1 - V_t) \log \lambda_t$ satisfies

$$\text{Var}[\hat{g}_0] - \text{Var}[\hat{g}_1] \geq (1 - \gamma^2) \sum_{t \in \mathcal{D}} (\log \lambda_t)^2 \cdot \text{Var}[h_t], \quad (19)$$

$$\text{where } \mathcal{D} = \{t : |\log \lambda_t| \geq \delta, V_t(1 - V_t) < \gamma\}.$$

Score vectors in autoregressive models are correlated across positions, so Eq. (19) is a directional indication rather than a quantitative guarantee, and the set \mathcal{D} expands once the model commits to a solution path, predicting larger gains on longer trajectories that are consistent with the stratified residual in Figure 1(c) and the length-stratified accuracy in Table 3(b).

4 OPPO: Oracle-Prompted Policy Optimization

The Bayesian value recursion of Section 3 is agnostic to how λ_t is estimated. The remainder of the section specifies the estimator, defines the prior V_0 , and the direction anchoring.

Oracle estimator. Computing λ_t requires scoring every sampled token both with and without y^* in context. In the *self-oracle* mode, the policy π_θ scores both contexts, adding one forward pass per trajectory and no extra model. In the *teacher-oracle* mode, a frozen π_ϕ replaces π_θ in both terms; π_ϕ receives no gradient updates and need not be instruction-tuned, since its role is likelihood scoring. The two modes operate at different points along the ϵ_t axis of Section 3.2, and once $\log \hat{\lambda}_{i,t}$ is computed every later step is identical, so the Bayesian machinery is decoupled from the choice of estimator.

Prior and ratio computation. Given G trajectories per query, the prior is the Beta(α, α) posterior mean, and ratios are clipped for numerical stability:

$$\hat{V}_0 = \frac{k + \alpha}{G + 2\alpha}, \quad \ell_0 = \log \frac{k + \alpha}{G - k + \alpha}, \quad \log \hat{\lambda}_{i,t} = \text{clip}(o_{i,t} - s_{i,t}, -C, C), \quad (20)$$

where $s_{i,t} = \log \hat{\pi}(y_{i,t} | x, y_{i,<t})$ and $o_{i,t} = \log \hat{\pi}(y_{i,t} | x, y^*, y_{i,<t})$. Setting $\alpha = 1$ keeps the log-odds finite in all-correct and all-incorrect groups, which would otherwise collapse every advantage to zero, while the clip bound C prevents a single extreme $\log \lambda_t$ from saturating ℓ_t and silencing later positions. The log-odds then accumulate as $\ell_{i,t} = \ell_0 + \sum_{j<t} \log \hat{\lambda}_{i,j}$ and the raw Bayesian advantage is $A_{i,t}^{\text{raw}} = \sigma(\ell_{i,t} + \log \hat{\lambda}_{i,t}) - \sigma(\ell_{i,t})$.

Table 1: Pass@1 accuracy (%) on reasoning benchmarks. All models are trained on DeepScaleR. OPPO variants are grouped by the underlying optimization framework and the oracle estimator. Subscript arrows denote improvement over the corresponding baseline.

Method	<i>Mathematical Reasoning</i>				<i>Scientific Reasoning</i>		<i>Code</i>
	GSM8K	MATH-500	AMC'23	AIME'24	GPQA-D	ARC-C	LCB
<i>Qwen3-4B-Instruct-2507</i>							
SFT	89.5	70.2	52.5	44.0	37.8	87.1	28.6
GRPO	91.4	72.8	54.0	46.4	39.2	88.0	31.5
Dr.GRPO	91.6	73.0	54.5	46.3	39.4	88.3	31.4
DAPO	92.3	74.2	55.8	47.0	40.3	88.5	32.8
SDPO	92.8	74.6	56.5	48.2	40.0	89.0	32.4
<i>on GRPO</i>							
Self-OPPO	93.0 _{↑1.6}	76.0 _{↑3.2}	58.5 _{↑4.5}	49.5 _{↑3.1}	41.6 _{↑2.4}	89.5 _{↑1.5}	34.2 _{↑2.7}
Teacher-OPPO	93.8 _{↑2.4}	77.4 _{↑4.6}	60.0 _{↑6.0}	51.3 _{↑4.9}	42.5 _{↑3.3}	89.8 _{↑1.8}	35.4 _{↑3.9}
<i>on DAPO</i>							
Self-OPPO	93.6 _{↑1.3}	76.8 _{↑2.6}	59.2 _{↑3.4}	50.0 _{↑3.0}	41.8 _{↑1.5}	89.6 _{↑1.1}	34.6 _{↑1.8}
Teacher-OPPO	94.5 _{↑2.2}	78.5 _{↑4.3}	61.5 _{↑5.7}	52.2 _{↑5.2}	43.2 _{↑2.9}	90.0 _{↑1.5}	36.2 _{↑3.4}
<i>Phi-4-mini-instruct</i>							
SFT	88.2	71.4	28.0	9.5	30.8	83.5	20.4
GRPO	89.8	75.0	32.5	12.0	32.4	84.6	23.0
Dr.GRPO	90.0	74.8	33.0	11.7	32.6	84.8	22.8
DAPO	90.5	76.2	34.0	13.3	33.5	85.0	24.2
SDPO	90.8	76.5	35.5	13.0	33.0	85.4	23.8
<i>on GRPO</i>							
Self-OPPO	91.4 _{↑1.6}	78.2 _{↑3.2}	37.0 _{↑4.5}	15.3 _{↑3.3}	34.5 _{↑2.1}	86.2 _{↑1.6}	25.8 _{↑2.8}
Teacher-OPPO	92.0 _{↑2.2}	80.0 _{↑5.0}	39.5 _{↑7.0}	17.0 _{↑5.0}	35.8 _{↑3.4}	86.8 _{↑2.2}	27.2 _{↑4.2}
<i>on DAPO</i>							
Self-OPPO	91.8 _{↑1.3}	78.8 _{↑2.6}	38.0 _{↑4.0}	16.0 _{↑2.7}	35.0 _{↑1.5}	86.4 _{↑1.4}	26.5 _{↑2.3}
Teacher-OPPO	92.5 _{↑2.0}	80.8 _{↑4.6}	40.5 _{↑6.5}	17.8 _{↑4.5}	36.4 _{↑2.9}	87.0 _{↑2.0}	28.0 _{↑3.8}

Direction anchoring. The sign of $A_{i,t}^{\text{raw}}$ is determined by $\log \lambda_t$, not by the trajectory outcome. Any token with $\log \lambda_t > 0$ in an incorrect trajectory would receive positive advantage and reinforce a flawed reasoning step, and tokens in correct trajectories with $\log \lambda_t < 0$ would be penalized despite contributing to a successful answer; the failure mode mirrors pure self-distillation, where the gradient direction follows the privileged teacher rather than the environment reward [35]. To prevent the inversion, OPPO anchors the sign of every token-level advantage to the sequence-level GRPO advantage and normalizes across the group:

$$\hat{A}_{i,t} = \text{sign}(A_i^{\text{seq}}) \cdot |A_{i,t}^{\text{raw}}|, \quad A_i^{\text{seq}} = \frac{R_i - \mu}{\sigma}, \quad \tilde{A}_{i,t} = \frac{\hat{A}_{i,t} - \bar{A}}{\sigma_A + \epsilon}. \quad (21)$$

The environment reward retains exclusive control over which trajectories are reinforced or penalized, while the Bayesian state weight and oracle evidence govern only the relative magnitude across positions within each trajectory.

Policy update. The normalized advantages enter the clipped surrogate objective

$$\mathcal{L}(\theta) = \mathbb{E} \left[\frac{1}{G} \sum_{i=1}^G \frac{1}{T_i} \sum_{t=1}^{T_i} \min \left(\rho_{i,t} \tilde{A}_{i,t}, \text{clip}(\rho_{i,t}, 1-\epsilon, 1+\epsilon) \tilde{A}_{i,t} \right) \right], \quad \rho_{i,t} = \frac{\pi_{\theta}(y_{i,t} | x, y_{i,<t})}{\pi_{\theta_{\text{old}}}(y_{i,t} | x, y_{i,<t})}. \quad (22)$$

Algorithm 1 summarizes the procedure that replace the uniform sequence-level advantage A_i^{seq} by the token-level $\hat{A}_{i,t}$, at the cost of one additional forward pass per trajectory.

5 Results

5.1 Experimental Setup

Models and data. We train all methods on DeepScaleR [26], approximately 40K problem-answer pairs drawn from AMC, AIME, MATH, and OlympiadBench. Each problem comes with a ground-truth integer answer that serves both as the verifiable reward and as the oracle context y^* for computing λ_t . We evaluate on two instruction-tuned models of comparable scale, Qwen3-4B-Instruct [34] and Phi-4-mini-instruct [1].

Benchmarks. For mathematical reasoning we use GSM8K [4], MATH-500 [22], AMC 2023¹, and AIME 2024 & 2025²; for scientific reasoning, GPQA-Diamond [28] and ARC-Challenge [3]; for code generation, LiveCodeBench [15]. None of the benchmarks overlap the training data, and Pass@1 accuracy is averaged over 16 sampling runs.

Comparison and configuration. Baselines are drawn from the GRPO family: GRPO [9], Dr.GRPO [24], DAPO [36], and SDPO [12]. We additionally apply OPPO on top of DAPO to isolate whether the Bayesian advantage adds gains beyond optimization mechanics. The teacher-oracle uses Qwen3-32B as the estimator π_ϕ for both base models. Experiments run on $2 \times$ H200 GPUs using the verl framework [30], with AdamW at learning rate 1×10^{-6} , batch size 32, group size $G = 8$, clip $\epsilon = 0.2$, evidence clip $C = 3.0$, and prior $\alpha = 1$.

5.2 Main Results

Table 1 reports performance across all seven benchmarks. Three findings organize the discussion.

Token-level credit improves reasoning. Self-OPPO outperforms GRPO and its optimization variants on every benchmark for both base models, with gains concentrated on competition-level tasks where reasoning chains are longest. The pattern matches the variance argument of Section 3.3: longer sequences accumulate more positions in determined regions where $V_t(1 - V_t) \approx 0$, and the Bayesian advantage suppresses gradient signal at the saturated positions while GRPO distributes credit uniformly. The further gains over SDPO, which leverages oracle-conditioned signals without cumulative belief tracking, indicate that the running state estimate adds headroom beyond per-token discrimination. **Oracle quality translates into training gains.** Teacher-OPPO improves over Self-OPPO on every benchmark, with the largest gains on the hardest tasks. Since the Bayesian machinery is identical in both variants, the improvement is attributable to sharper λ_t estimates from the larger oracle. Scoring student tokens under a 32B model approximates a controlled distillation signal, so the additional gains over Self-OPPO should be read as evidence that the framework absorbs higher-quality λ_t rather than as a within-model improvement at fixed scale; Self-OPPO remains the cleaner test of the Bayesian mechanism. **The Bayesian advantage complements optimization improvements.** OPPO on top of DAPO yields gains comparable in magnitude to OPPO on GRPO, and Teacher-OPPO on DAPO reaches the highest performance on most benchmarks for both models. Improved clipping and filtering are therefore complementary to finer credit assignment rather than redundant with it.

5.3 Ablation and Analysis

Table 2 removes each component of Self-OPPO individually on Qwen3-4B-Instruct. Direction anchoring is the most important: tokens in incorrect trajectories that correlate with y^* produce $\log \lambda_t > 0$ and receive positive advantage, reinforcing flawed reasoning, and AIME’24 performance falls below GRPO without anchoring, mirroring the degradation of pure self-distillation [35]. State

Algorithm 1 Oracle-Prompted Policy Optimization

Require: Policy π_θ , oracle estimator π_{est} (π_θ or π_ϕ), group size G , prior α , clip C

- 1: **for** each query x with answer y^* **do**
- 2: *# Rollout and reward*
- 3: Sample $\{y^{(i)}\}_{i=1}^G \sim \pi_\theta(\cdot | x)$
- 4: Obtain R_i ; $A_i^{\text{seq}} \leftarrow (R_i - \mu) / \sigma$
- 5: $k \leftarrow \sum_i R_i$; $\ell_0 \leftarrow \log \frac{k + \alpha}{G - k + \alpha}$
- 6: *# Oracle evaluation*
- 7: **for** $i = 1, \dots, G$ **do**
- 8: $s_t \leftarrow \log \pi_{\text{est}}(y_{i,t} | x, y_{i,<t})$
- 9: $o_t \leftarrow \log \pi_{\text{est}}(y_{i,t} | x, y^*, y_{i,<t})$
- 10: $\log \hat{\lambda}_{i,t} \leftarrow \text{clip}(o_t - s_t, -C, C)$
- 11: **end for**
- 12: *# Bayesian credit assignment*
- 13: **for** $i = 1, \dots, G$ **do**
- 14: $\ell_{i,t} \leftarrow \ell_0 + \sum_{j<t} \log \hat{\lambda}_{i,j}$
- 15: $A_{i,t}^{\text{raw}} \leftarrow \sigma(\ell_{i,t} + \log \hat{\lambda}_{i,t}) - \sigma(\ell_{i,t})$
- 16: $\hat{A}_{i,t} \leftarrow \text{sign}(A_i^{\text{seq}}) \cdot |A_{i,t}^{\text{raw}}|$
- 17: **end for**
- 18: $\bar{A}_{i,t} \leftarrow (\hat{A}_{i,t} - \bar{A}) / (\sigma_A + \epsilon)$
- 19: **end for**
- 20: *# Policy update*
- 21: Update θ via Eq. (22)

¹<https://huggingface.co/datasets/AI-MO/aimo-validation-amc>

²<https://huggingface.co/datasets/AI-MO/aimo-validation-aime>

Table 3: (a) Oracle estimator capacity: performance rises monotonically with teacher scale, with the largest jump at the 4B-to-8B transition and near-saturated gains beyond. All teachers are Qwen3 base models. (b) OPPO gains widen with sequence length as more tokens enter determined regions.

(a) Oracle estimator capacity				(b) Accuracy by response length				
Estimator	Size	M-500	AIME'24	Method	0–256	257–512	513–1024	1025+
Self	4B	76.0	49.5	GRPO	88.5	80.2	68.4	52.0
Qwen3-8B	8B	76.8	50.2	SDPO	89.0	81.5	70.8	55.2
Qwen3-14B	14B	77.0	50.8	Self-OPPO	89.2	82.0	73.5	62.8
Qwen3-32B	32B	77.4	51.3					

tracking ranks second, with the largest drops on AMC and AIME'24 where reasoning chains are longest: without the $V_t(1 - V_t)$ factor, every position receives weight proportional to $|\log \lambda_t|$ regardless of trajectory commitment, and longer chains accumulate more saturated positions. The "log λ_t -only" row, which removes both state tracking and clipping, sits close to GRPO across the four benchmarks; the gap to the full method quantifies the joint contribution of state tracking and numerical control, while the small margin over GRPO, negligible on AIME'24, isolates the value of per-token oracle evidence on its own.

Table 2: Component ablation on Qwen3-4B-Instruct-2507, concentrated on long-chain benchmarks.

Configuration	M-500	AMC	AIME'24	GPQA
Self-OPPO (full)	76.0	58.5	49.5	41.6
remove anchoring	71.8	51.0	43.0	38.5
remove tracking	74.5	55.8	46.8	40.0
remove clipping	75.4	57.5	48.6	41.2
remove prior	75.8	58.0	49.0	41.5
log λ_t only	73.6	55.0	46.5	39.8
GRPO (uniform)	72.8	54.0	46.4	39.2

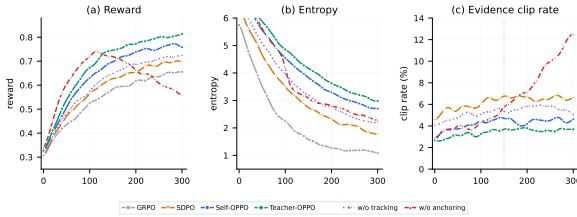


Figure 2: Without anchoring, reward collapses after step 150 as the clip rate diverges. Removing state tracking reduces the entropy preservation that separates OPPO from other methods.

quality λ_t and that the estimator needs only next-token prediction capability rather than instruction-following ability. Table 3(b) partitions MATH-500 by response length: all three methods perform comparably on the shortest bin because V_t stays near V_0 , while the gap widens with length and Self-OPPO shows the largest separation in the longest bin, matching the prediction of Section 3.3 that variance reduction grows with $|\mathcal{D}|$. Hyperparameter sensitivity and token-level credit visualizations are in Appendix H.

6 Conclusion

OPPO recovers token-level advantages by accumulating oracle-conditioned likelihood ratios into a running Bayesian estimate of trajectory success, concentrating credit where the outcome remains uncertain and adding no learned components beyond one extra forward pass. Experiments across mathematical, scientific, and code reasoning benchmarks confirm consistent gains that widen on longer sequences, with stronger oracle estimators yielding monotonically better performance. Extending the framework beyond domains with verifiable answers remains an open direction, as does adapting the Bayesian recursion to richer outcome signals such as partial-credit rubrics.

References

- [1] Marah Abdin, Sahaj Agarwal, Ahmed Awadallah, Vidhisha Balachandran, Harkirat Behl, Lingjiao Chen, Gustavo de Rosa, Suriya Gunasekar, Mojan Javaheripi, Neel Joshi, et al. Phi-4-reasoning technical report. *arXiv preprint arXiv:2504.21318*, 2025.
- [2] Rishabh Agarwal, Nino Vieillard, Yongchao Zhou, Piotr Stanczyk, Sabela Ramos Garea, Matthieu Geist, and Olivier Bachem. On-policy distillation of language models: Learning from self-generated mistakes. In *The twelfth international conference on learning representations*, 2024.
- [3] Peter Clark, Isaac Cowhey, Oren Etzioni, Tushar Khot, Ashish Sabharwal, Carissa Schoenick, and Oyvind Tafjord. Think you have solved question answering? try arc, the ai2 reasoning challenge. *arXiv:1803.05457v1*, 2018.
- [4] Karl Cobbe, Vineet Kosaraju, Mohammad Bavarian, Mark Chen, Heewoo Jun, Lukasz Kaiser, Matthias Plappert, Jerry Tworek, Jacob Hilton, Reiichiro Nakano, Christopher Hesse, and John Schulman. Training verifiers to solve math word problems. *arXiv preprint arXiv:2110.14168*, 2021.
- [5] Karl Cobbe, Vineet Kosaraju, Mohammad Bavarian, Mark Chen, Heewoo Jun, Lukasz Kaiser, Matthias Plappert, Jerry Tworek, Jacob Hilton, Reiichiro Nakano, et al. Training verifiers to solve math word problems. *arXiv preprint arXiv:2110.14168*, 2021.
- [6] Ganqu Cui, Lifan Yuan, Zefan Wang, Hanbin Wang, Yuchen Zhang, Jiacheng Chen, Wendi Li, Bingxiang He, Yuchen Fan, Tianyu Yu, et al. Process reinforcement through implicit rewards. *arXiv preprint arXiv:2502.01456*, 2025.
- [7] Mohammad Ghavamzadeh, Shie Mannor, Joelle Pineau, and Aviv Tamar. Bayesian reinforcement learning: A survey. *Foundations and Trends® in Machine Learning*, 8(5-6):359–483, 2015.
- [8] Yuxian Gu, Li Dong, Furu Wei, and Minlie Huang. Minillm: Knowledge distillation of large language models. *arXiv preprint arXiv:2306.08543*, 2023.
- [9] Daya Guo, Dejian Yang, Haowei Zhang, Junxiao Song, Peiyi Wang, Qihao Zhu, Runxin Xu, Ruoyu Zhang, Shirong Ma, Xiao Bi, et al. Deepseek-r1: Incentivizing reasoning capability in llms via reinforcement learning. *arXiv preprint arXiv:2501.12948*, 2025.
- [10] Yiran Guo, Lijie Xu, Jie Liu, Dan Ye, and Shuang Qiu. Segment policy optimization: Effective segment-level credit assignment in rl for large language models. *arXiv preprint arXiv:2505.23564*, 2025.
- [11] Zhenyu Hou, Ziniu Hu, Yujiang Li, Rui Lu, Jie Tang, and Yuxiao Dong. Treerl: Llm reinforcement learning with on-policy tree search. In *Proceedings of the 63rd Annual Meeting of the Association for Computational Linguistics (Volume 1: Long Papers)*, pages 12355–12369, 2025.
- [12] Jonas Hübner, Frederike Lübeck, Lejs Behric, Anton Baumann, Marco Bagatella, Daniel Marta, Ido Hakimi, Idan Shenfeld, Thomas Kleine Buening, Carlos Guestrin, et al. Reinforcement learning via self-distillation. *arXiv preprint arXiv:2601.20802*, 2026.
- [13] Aaron Jaech, Adam Kalai, Adam Lerer, Adam Richardson, Ahmed El-Kishky, Aiden Low, Alec Helyar, Aleksander Madry, Alex Beutel, Alex Carney, et al. Openai o1 system card. *arXiv preprint arXiv:2412.16720*, 2024.
- [14] Adit Jain and Brendan Rappazzo. Learning to reason with mixture of tokens. *arXiv preprint arXiv:2509.21482*, 2025.
- [15] Naman Jain, King Han, Alex Gu, Wen-Ding Li, Fanjia Yan, Tianjun Zhang, Sida Wang, Armando Solar-Lezama, Koushik Sen, and Ion Stoica. Livecodebench: Holistic and contamination free evaluation of large language models for code. *arXiv preprint arXiv:2403.07974*, 2024.
- [16] Samyak Jain, Ayush Agrawal, and Navin Goyal. Towards understanding the optimization landscape of grpo and its variants. In *First Workshop on Foundations of Reasoning in Language Models*, 2025.

- [17] Michael I Jordan, Zoubin Ghahramani, Tommi S Jaakkola, and Lawrence K Saul. An introduction to variational methods for graphical models. *Machine learning*, 37(2):183–233, 1999.
- [18] Rudolph Emil Kalman. A new approach to linear filtering and prediction problems. 1960.
- [19] Amirhossein Kazemnejad, Milad Aghajohari, Eva Portelance, Alessandro Sordoni, Siva Reddy, Aaron Courville, and Nicolas Le Roux. Vineppo: Unlocking rl potential for llm reasoning through refined credit assignment. 2024.
- [20] Maxim Khanov, Jirayu Burapachee, and Yixuan Li. Args: Alignment as reward-guided search. *arXiv preprint arXiv:2402.01694*, 2024.
- [21] Yu Li, Sizhe Tang, and Tian Lan. Reason in chains, learn in trees: Self-rectification and grafting for multi-turn agent policy optimization. *arXiv preprint arXiv:2604.07165*, 2026.
- [22] Hunter Lightman, Vineet Kosaraju, Yura Burda, Harri Edwards, Bowen Baker, Teddy Lee, Jan Leike, John Schulman, Ilya Sutskever, and Karl Cobbe. Let’s verify step by step. *arXiv preprint arXiv:2305.20050*, 2023.
- [23] Zheng Liu, Mengjie Liu, Siwei Wen, Mengzhang Cai, Bin Cui, Conghui He, and Wentao Zhang. From uniform to heterogeneous: Tailoring policy optimization to every token’s nature. *arXiv preprint arXiv:2509.16591*, 2025.
- [24] Zichen Liu, Changyu Chen, Wenjun Li, Penghui Qi, Tianyu Pang, Chao Du, Wee Sun Lee, and Min Lin. Understanding r1-zero-like training: A critical perspective. *arXiv preprint arXiv:2503.20783*, 2025.
- [25] Kevin Lu and Thinking Machines Lab. On-policy distillation. *Thinking Machines Lab: Connectionism*, 2025. doi: 10.64434/tml.20251026. <https://thinkingmachines.ai/blog/on-policy-distillation>.
- [26] Michael Luo, Sijun Tan, Justin Wong, Xiaoxiang Shi, William Tang, Manan Roongta, Colin Cai, Jeffrey Luo, Tianjun Zhang, Erran Li, Raluca Ada Popa, and Ion Stoica. Deepscaler: Surpassing o1-preview with a 1.5b model by scaling rl, 2025. Notion Blog.
- [27] Avinash Patil and Aryan Jadon. Advancing reasoning in large language models: Promising methods and approaches. *arXiv preprint arXiv:2502.03671*, 2025.
- [28] David Rein, Betty Li Hou, Asa Cooper Stickland, Jackson Petty, Richard Yuanzhe Pang, Julien Dirani, Julian Michael, and Samuel R Bowman. Gpqa: A graduate-level google-proof q&a benchmark. In *First conference on language modeling*, 2024.
- [29] John Schulman, Filip Wolski, Prafulla Dhariwal, Alec Radford, and Oleg Klimov. Proximal policy optimization algorithms. *arXiv preprint arXiv:1707.06347*, 2017.
- [30] Guangming Sheng, Chi Zhang, Zilingfeng Ye, Xibin Wu, Wang Zhang, Ru Zhang, Yanghua Peng, Haibin Lin, and Chuan Wu. Hybridflow: A flexible and efficient rlhf framework. In *Proceedings of the Twentieth European Conference on Computer Systems*, pages 1279–1297, 2025.
- [31] Mingyang Song and Mao Zheng. A survey of on-policy distillation for large language models. *arXiv preprint arXiv:2604.00626*, 2026.
- [32] Jiankai Sun, Chuanyang Zheng, Enze Xie, Zhengying Liu, Ruihang Chu, Jianing Qiu, Jiaqi Xu, Mingyu Ding, Hongyang Li, Mengzhe Geng, et al. A survey of reasoning with foundation models: Concepts, methodologies, and outlook. *ACM Computing Surveys*, 57(11):1–43, 2025.
- [33] Richard S Sutton. Learning to predict by the methods of temporal differences. *Machine learning*, 3(1):9–44, 1988.
- [34] An Yang, Anfeng Li, Baosong Yang, Beichen Zhang, Binyuan Hui, Bo Zheng, Bowen Yu, Chang Gao, Chengen Huang, Chenxu Lv, et al. Qwen3 technical report. *arXiv preprint arXiv:2505.09388*, 2025.

- [35] Chenxu Yang, Chuanyu Qin, Qingyi Si, Minghui Chen, Naibin Gu, Dingyu Yao, Zheng Lin, Weiping Wang, Jiaqi Wang, and Nan Duan. Self-distilled rlvr. *arXiv preprint arXiv:2604.03128*, 2026.
- [36] Qiyang Yu, Zheng Zhang, Ruofei Zhu, Yufeng Yuan, Xiaochen Zuo, Yu Yue, Weinan Dai, Tiantian Fan, Gaohong Liu, Lingjun Liu, et al. Dapo: An open-source llm reinforcement learning system at scale. *arXiv preprint arXiv:2503.14476*, 2025.
- [37] Siyan Zhao, Zhihui Xie, Mengchen Liu, Jing Huang, Guan Pang, Feiyu Chen, and Aditya Grover. Self-distilled reasoner: On-policy self-distillation for large language models. *arXiv preprint arXiv:2601.18734*, 2026.
- [38] Yuzhong Zhao, Yue Liu, Junpeng Liu, Jingye Chen, Xun Wu, Yaru Hao, Tengchao Lv, Shaohan Huang, Lei Cui, Qixiang Ye, et al. Geometric-mean policy optimization. *arXiv preprint arXiv:2507.20673*, 2025.
- [39] Chujie Zheng, Shixuan Liu, Mingze Li, Xiong-Hui Chen, Bowen Yu, Chang Gao, Kai Dang, Yuqiong Liu, Rui Men, An Yang, et al. Group sequence policy optimization. *arXiv preprint arXiv:2507.18071*, 2025.

A Extended Related Work

This appendix expands the discussion in Section 1 along three axes that frame OPPO within the broader landscape of credit assignment and reinforcement learning for reasoning. The body section establishes the immediate baselines; here we situate the framework against the wider literature.

A.1 Trajectory-Level Optimization and Critic-Based Alternatives

Group Relative Policy Optimization [9] and its descendants form the dominant on-policy paradigm for reasoning. Dr.GRPO [24] fixes the reference policy in the importance ratio denominator to remove the length-bias of the original objective. DAPO [36] introduces asymmetric clipping and filtered sampling. GSPO [39] aggregates probabilities at the sequence level. GMPO [38] replaces the arithmetic-mean group baseline with a geometric mean. Across these variants, the per-token advantage remains a single trajectory-level scalar broadcast uniformly across positions [10], which is the limitation that motivates OPPO. The Bayesian recursion of Section 3 is orthogonal to the optimization-mechanic improvements, and Section 5 shows that applying OPPO on top of DAPO yields gains comparable in magnitude to applying it over standard GRPO.

The critic-based alternative is Proximal Policy Optimization [29], which pairs the clipped surrogate with a learned value network $V_\phi(s_t)$ that approximates the on-policy state value of Eq. (3) via temporal-difference regression. VinePPO[19] show that the learned critic in PPO barely outperforms a random baseline on long-horizon reasoning trajectories, where credit-assignment difficulty grows with sequence length and the regression target is dominated by sparse outcome rewards. The Bayesian value recursion of Section 3 can be read as an analytical alternative to fitting V_ϕ : rather than learning the success probability through bootstrapped regression targets, the recursion computes it in closed form from the per-token oracle ratio, with the running posterior V_t playing the role of V_ϕ at no parameter cost.

A.2 Critic-Free Token-Level Credit and Distillation-Based Methods

Beyond GRPO and PPO, several critic-free approaches resolve credit at finer granularity than the trajectory level. VinePPO [19] estimates per-step values through Monte Carlo rollouts that branch from each prefix; the estimator is unbiased but requires orders-of-magnitude more inference. TreeRL [11] extends the tree-search idea to multi-branch rollouts. PRIME [6] trains an implicit process reward model that supplies dense token-level rewards but requires online updating to avoid reward hacking. Segment Policy Optimization [10] aggregates descendant outcomes within shared prefixes, sitting between trajectory-level and token-level granularity. Process reward models more broadly [22] train a separate verifier to score intermediate reasoning steps. Compared with all such methods, OPPO achieves token-level resolution at the cost of one extra forward pass per trajectory and without any auxiliary network or rollout, by exploiting the privileged y^* context to derive a closed-form per-token signal. The trade-off is that OPPO requires verifiable training-time answers; methods that use Monte Carlo rollouts, learned critics, or step verifiers do not.

The line of work most closely related to OPPO uses on-policy distillation [2, 8, 25] with a privileged teacher. The reasoning-specific variant conditions the teacher on the ground-truth answer [37, 12]: RLSD [35] and SDPO [12] use the resulting answer-conditioned likelihood ratio as a token-level reward within GRPO. As established in Section 2.2, the per-token signal $\log \lambda_t$ is the same quantity in all four works; the substantive distinction is what OPPO does with the signal. Where SDPO and RLSD apply $\log \lambda_t$ as an isolated per-token reward with uniform weight, OPPO accumulates it through the Bayesian recursion of Eq. (10) and modulates each contribution by the running state weight $V_t(1 - V_t)$. Section 5 shows that the additional Bayesian machinery yields consistent improvements over SDPO across all benchmarks, with the largest gains on long-chain competition-mathematics tasks where the state weight has the most room to redistribute credit.

A.3 Methodological Connections

The recursion of Section 3.1 is structurally a Bayesian filter over a binary latent variable (eventual success), with the per-token oracle ratio playing the role of the observation likelihood. The closed-form additivity in log-odds space is a standard property of Bayes’ rule applied to binary outcomes [18, 17]. The novelty is not the filter itself but its identification with token-level RL credit assignment:

the running posterior V_t coincides with the success probability targeted by the on-policy state value of Eq. (3), and the one-step posterior change $V_{t+1} - V_t$ recovers the temporal-difference advantage $A_t = Q_t - V_t$ in the perfect-oracle limit. The connection to TD learning [33] is that OPPO provides an analytical, non-bootstrapped value estimator in a regime where bootstrapping is expensive (full reasoning rollout) and the target signal is sparse (binary terminal reward). Bayesian RL methods that maintain explicit posterior beliefs over reward or value functions [7] typically require either conjugate priors or posterior-sampling machinery; the closed-form structure of the binary-outcome posterior here sidesteps both. The framework is therefore best understood as a Bayesian filtering interpretation of the existing on-policy distillation primitive, not as a fully Bayesian reinforcement-learning method.

A separate line of work uses learned or implicit value estimates to guide decoding at inference time, including verifier-augmented decoding [5] and value-guided sampling [20]. OPPO operates entirely at training time: it modifies how trajectory-level reward is redistributed across tokens during gradient updates, and the deployed policy uses no oracle context, no verifier, and no tree search. The interpretation of V_t as a running success probability does, however, suggest a natural inference-time analogue: the same recursion could in principle be applied with a self-oracle estimator at decoding time to weight token candidates by their belief contribution. Such a use of the framework is outside the scope of this paper and is left for future work. We note also that token-level credits learned via OPPO at training time may align with regions where verifier-guided decoding methods place high mass at inference, since both quantities track the model’s running belief about eventual success; an empirical correlation analysis is similarly outside scope.

B Detailed Derivations

B.1 Bayesian Update Derivation

The full derivation of the value recursion proceeds from the definition $V_t = P(R=1 \mid x, y_{1:t-1})$. Bayes’ theorem gives the posterior after observing y_t :

$$V_{t+1} = P(R=1 \mid x, y_{1:t}) = \frac{P(y_t \mid x, y_{<t}, R=1) \cdot V_t}{P(y_t \mid x, y_{<t})}. \quad (23)$$

The denominator expands by the law of total probability,

$$P(y_t \mid x, y_{<t}) = P(y_t \mid x, y_{<t}, R=1) V_t + P(y_t \mid x, y_{<t}, R=0) (1 - V_t). \quad (24)$$

Substituting Modeling Choice 3.2 into the numerator and Modeling Choice 3.2 into the second denominator term, then dividing numerator and denominator by $\pi(y_t \mid x, y_{<t})$, yields

$$V_{t+1} = \frac{\lambda_t V_t}{\lambda_t V_t + (1 - V_t)}, \quad \lambda_t = \frac{\pi_{\text{est}}(y_t \mid x, y_{<t}, y^*)}{\pi_{\text{est}}(y_t \mid x, y_{<t})}, \quad (25)$$

which is exactly the same expression in the main text.

B.2 Logit-Space Reduction

Define the running log-odds $\ell_t = \log \frac{V_t}{1-V_t}$. From Eq. (25),

$$\frac{V_{t+1}}{1 - V_{t+1}} = \frac{\lambda_t V_t / (\lambda_t V_t + 1 - V_t)}{(1 - V_t) / (\lambda_t V_t + 1 - V_t)} = \frac{\lambda_t V_t}{1 - V_t} = \lambda_t \cdot \frac{V_t}{1 - V_t}, \quad (26)$$

so taking logarithms collapses the multiplicative recursion in V_t to additive accumulation in ℓ_t :

$$\ell_{t+1} = \log \lambda_t + \ell_t, \quad \ell_t = \ell_0 + \sum_{i=1}^{t-1} \log \lambda_i, \quad V_t = \sigma(\ell_t) = \frac{1}{1 + e^{-\ell_t}}. \quad (27)$$

B.3 Advantage Closed Form

The token-level advantage $A_t = V_{t+1} - V_t$ admits a closed-form expression. Subtracting V_t from Eq. (25) and clearing the common denominator,

$$A_t = \frac{\lambda_t V_t - V_t(\lambda_t V_t + 1 - V_t)}{\lambda_t V_t + 1 - V_t} = \frac{\lambda_t V_t - \lambda_t V_t^2 - V_t + V_t^2}{\lambda_t V_t + 1 - V_t} = \frac{V_t(1 - V_t)(\lambda_t - 1)}{\lambda_t V_t + 1 - V_t}. \quad (28)$$

The first-order approximation follows from two small-quantity expansions when $|\lambda_t - 1| \ll 1$. The denominator satisfies $\lambda_t V_t + 1 - V_t = 1 + (\lambda_t - 1)V_t \approx 1$, and the numerator satisfies $\lambda_t - 1 \approx \log \lambda_t$ via the Taylor expansion $e^x - 1 \approx x$. Substituting both gives

$$A_t \approx V_t(1 - V_t) \cdot \log \lambda_t, \quad (29)$$

which is Eq. (18) in the main text.

B.4 Telescoping Property

Using the identity $A_t = \sigma(\ell_{t+1}) - \sigma(\ell_t)$ established, the trajectory sum telescopes:

$$\sum_{t=1}^T A_t = \sum_{t=1}^T [\sigma(\ell_{t+1}) - \sigma(\ell_t)] = \sigma(\ell_{T+1}) - \sigma(\ell_1). \quad (30)$$

At the terminal state, the Bayesian posterior should converge to $V_{T+1} = R$, giving $\sigma(\ell_{T+1}) = R$ in the limit of an unconstrained recursion. With $\sigma(\ell_1) = V_0$ at the start, the budget identity becomes

$$\sum_{t=1}^T A_t \approx R - V_0. \quad (31)$$

Evidence clipping prevents ℓ_{T+1} from reaching $\pm\infty$ in practice, so $\sigma(\ell_{T+1})$ approximates rather than equals R . The empirical residual on 200 MATH-500 trajectories has mean 0.007 and 95th percentile 0.018 (Figure 1(c)), confirming that the deviation from the exact identity is small in aggregate.

B.5 Lipschitz and Range Bounds on the Advantage

The sigmoid derivative satisfies $\sigma'(x) = \sigma(x)(1 - \sigma(x)) \leq \frac{1}{4}$ for all x , with equality at $x = 0$. The mean value theorem applied to σ yields the Lipschitz bound, while the fact that σ maps \mathbb{R} into the open interval $(0, 1)$ yields a universal range bound:

$$|A_t| = |\sigma(\ell_t + \log \lambda_t) - \sigma(\ell_t)| \leq \frac{1}{4} |\log \lambda_t|, \quad |A_t| < 1 \text{ for any } \ell_t, \log \lambda_t \in \mathbb{R}. \quad (32)$$

The two combine to give $|A_t| \leq \min(\frac{1}{4} |\log \lambda_t|, 1)$, with the Lipschitz bound active when $|\log \lambda_t| < 4$ and the range bound active otherwise. With evidence clipping $|\log \hat{\lambda}_t| \leq C$, the per-token contribution is further bounded by $|A_t| \leq \min(C/4, 1)$. For the manuscript’s choice $C = 3.0$, the Lipschitz bound is binding and gives $|A_t| \leq 0.75$.

C Variance Reduction Proof

We provide the full derivation of the bound in Eq. (19), with the caveat already noted in Section 3.3: the uncorrelated-score-vector assumption does not hold for autoregressive language models, so the bound should be read as a directional indication rather than a quantitative guarantee on practical training runs.

Proposition 1. *Let $\hat{g} = \sum_{t=1}^T w_t h_t$ denote the policy gradient estimator, where $h_t = \nabla_{\theta} \log \pi_{\theta}(y_t | x, y_{<t})$ is the score vector at position t . Suppose $\text{Cov}[h_s, h_t] = 0$ for all $s \neq t$, and consider two weighting schemes,*

$$w_t^{\text{blind}} = \log \lambda_t, \quad w_t^{\text{Bayes}} = V_t(1 - V_t) \log \lambda_t.$$

Then $\text{Var}[\hat{g}^{\text{blind}}] \geq \text{Var}[\hat{g}^{\text{Bayes}}]$, with the gap bounded below by

$$\text{Var}[\hat{g}^{\text{blind}}] - \text{Var}[\hat{g}^{\text{Bayes}}] \geq (1 - \gamma^2) \sum_{t \in T_{\text{det}}} (\log \lambda_t)^2 \text{Var}[h_t], \quad T_{\text{det}} = \{t : |\log \lambda_t| \geq \delta, V_t(1 - V_t) < \gamma\}, \quad (33)$$

for any thresholds $\delta, \gamma > 0$.

Proof. Under the uncorrelated-score assumption, the variance of each estimator decomposes additively across positions:

$$\text{Var}[\hat{g}^{\text{blind}}] = \sum_{t=1}^T (\log \lambda_t)^2 \text{Var}[h_t], \quad \text{Var}[\hat{g}^{\text{Bayes}}] = \sum_{t=1}^T V_t^2 (1 - V_t)^2 (\log \lambda_t)^2 \text{Var}[h_t]. \quad (34)$$

The variance gap is therefore

$$\Delta = \text{Var}[\hat{g}^{\text{blind}}] - \text{Var}[\hat{g}^{\text{Bayes}}] = \sum_{t=1}^T [1 - V_t^2(1 - V_t)^2] (\log \lambda_t)^2 \text{Var}[h_t]. \quad (35)$$

Since $V_t \in [0, 1]$ implies $V_t(1 - V_t) \leq \frac{1}{4}$, every factor satisfies $V_t^2(1 - V_t)^2 \leq \frac{1}{16}$, so $1 - V_t^2(1 - V_t)^2 \geq \frac{15}{16} > 0$ and $\Delta \geq 0$. To obtain the interpretable lower bound, restrict the sum to T_{det} and use $V_t^2(1 - V_t)^2 < \gamma^2$ on that subset:

$$\Delta \geq \sum_{t \in T_{\text{det}}} [1 - V_t^2(1 - V_t)^2] (\log \lambda_t)^2 \text{Var}[h_t] \geq (1 - \gamma^2) \sum_{t \in T_{\text{det}}} (\log \lambda_t)^2 \text{Var}[h_t]. \quad (36) \quad \square$$

The bound is informative when T_{det} is large, which happens in two regimes. The first is long sequences, where V_t saturates after a pivotal decision and many subsequent positions retain nonzero $\log \lambda_t$ from answer-correlated content. The second is easy or unsolvable queries, where V_0 already sits near 0 or 1 before any tokens are generated, so $V_t(1 - V_t) \approx 0$ throughout the trajectory while $\log \lambda_t$ remains nonzero. In both regimes the Bayesian state weight collapses to near zero on the saturating positions, so the corresponding gradient contributions are suppressed in \hat{g}^{Bayes} but not in \hat{g}^{blind} . The empirical sequence-length stratification in Table 3(b) is consistent with the predicted pattern: the gap between Self-OPPO and the state-blind baselines widens monotonically with response length.

D Oracle Quality Analysis

D.1 Bias Under Imperfect Oracle

When $\epsilon_t > 0$, the estimated λ_t differs from the true posterior ratio. The deviation has a clean interpretation. Let $p_t = P(y_t | x, y_{<t}, R=1)$ denote the true success-conditional probability and $q_t = \pi_{\text{est}}(y_t | x, y_{<t}, y^*)$ the oracle estimate. Define the true ratio λ_t^* and the estimated ratio $\hat{\lambda}_t$ on the same denominator:

$$\lambda_t^* = \frac{p_t}{\pi(y_t | x, y_{<t})}, \quad \hat{\lambda}_t = \frac{q_t}{\pi(y_t | x, y_{<t})}, \quad \log \hat{\lambda}_t - \log \lambda_t^* = \log q_t - \log p_t. \quad (37)$$

The KL definition $\epsilon_t = \mathbb{E}_{y_t \sim p_t} [\log p_t - \log q_t]$ gives the expected log-ratio bias under the true success-conditional distribution:

$$\mathbb{E}_{y_t \sim p_t} [\log \hat{\lambda}_t - \log \lambda_t^*] = -\epsilon_t. \quad (38)$$

The bias is non-positive on average, so the oracle estimate is conservative and underestimates the true evidence for success. Stronger oracles reduce ϵ_t and the magnitude of the bias, which is consistent with the monotonic improvement in Table 3(a).

D.2 Why Same-Family Teachers Are Preferred

The oracle quality ϵ_t depends not only on model capacity but also on distributional alignment between the estimator and the true posterior. Cross-family teachers, for example a Llama model scoring Qwen trajectories, can produce large ϵ_t despite high capacity because tokenization, positional encoding, and pre-training corpus all differ. The ratio structure $\log \lambda_t = \log \pi_{\text{est}}(y_t | x, y_{<t}, y^*) - \log \pi_{\text{est}}(y_t | x, y_{<t})$ cancels many model-specific biases through subtraction, but residual mismatch in the conditional shape still inflates ϵ_t . Same-family, larger-scale models are the recommended choice for the teacher-oracle role because the cancellation is most effective when the two scoring distributions share the same underlying parameterization.

E Connection to Distillation

E.1 On-Policy Distillation as a Special Case

Section 2.2 introduced the on-policy distillation objective \mathcal{L}_{OPD} with the oracle-conditioned teacher $\pi_T(\cdot | x, y_{<t}) \equiv \pi_{\text{est}}(\cdot | x, y_{<t}, y^*)$, and showed that the per-token gradient at the sampled token

y_t reduces to a policy-gradient form with weight $\log \lambda_t$. Repeating the conclusion in the present notation,

$$\nabla_{\theta} \mathcal{L}_{\text{OPD}}(\theta) \Big|_{y_t} = -\log \lambda_t \cdot \nabla_{\theta} \log \pi_{\theta}(y_t | x, y_{<t}), \quad \log \lambda_t = \log \pi_{\text{est}}(y_t | x, y_{<t}, y^*) - \log \pi_{\theta}(y_t | x, y_{<t}). \quad (39)$$

Pure on-policy distillation is therefore a policy gradient with advantage $\log \lambda_t$, identical to the "log λ_t only" row of the ablation in Table 2. The Bayesian advantage in Eq. (18) differs from the distillation gradient in two specific ways. The state weight $V_t(1 - V_t)$ concentrates the gradient on positions where the outcome remains uncertain, so determined regions receive negligible updates. Direction anchoring binds the sign of every token-level advantage to the sequence-level GRPO advantage, so the environment reward retains exclusive control over which trajectories are reinforced or penalized. The two modifications are independent: removing either one degrades performance, but the failure mechanisms differ, as documented in the ablation analysis of Section 5.

E.2 Spectrum of Methods

The factorization $A_t \approx V_t(1 - V_t) \cdot \log \lambda_t$ organizes a spectrum of methods along three axes: the per-token signal carried into the gradient, whether a state-tracking factor weights the signal, and which quantity controls the sign of each trajectory’s update.

Table 4: Method spectrum induced by the Bayesian factorization. Each row corresponds to one column setting in the ablation of Table 2: GRPO matches "uniform"; SDPO matches "log λ_t only" with environment-anchored direction; pure distillation (OPSD) matches "remove anchoring".

Method	Per-token signal	State tracking	Direction
GRPO [9]	uniform A_t^{seq}	—	environment reward
Anchored distillation (SDPO) [12]	$ \log \lambda_t $	—	environment reward
Self-OPPO (ours)	$V_t(1 - V_t) \log \lambda_t $	Bayesian	environment reward
Teacher-OPPO (ours)	$V_t(1 - V_t) \log \lambda_t $, lower ϵ_t	Bayesian	environment reward
Pure distillation (OPSD) [37]	$\log \lambda_t$	—	teacher

Reading the table from top to bottom moves through the design space. GRPO sits at the trajectory-level extreme, with no per-token discrimination and no state tracking. Anchored distillation introduces $\log \lambda_t$ as a per-token signal but applies it uniformly across positions. OPPO adds the Bayesian state weight $V_t(1 - V_t)$, modulating the per-token signal by the running belief about success. The self-oracle and teacher-oracle variants of OPPO differ only in the quality of the $\log \lambda_t$ estimate, parameterized by ϵ_t . Pure distillation drops direction anchoring and lets $\log \lambda_t$ control the sign of the update, which is the failure mode reproduced in the "remove anchoring" row of Table 2.

F Extended Experimental Results

F.1 Full Results on Phi-4-mini

Table 5 reports the complete results for Phi-4-mini across all benchmarks and ablation configurations, complementing the Qwen3-4B results in the main text. The pattern matches the Qwen3-4B case: OPPO improves over every baseline on every benchmark, with the largest absolute gains on AIME’24 and the largest relative gains on competition-level tasks where the base model is weakest.

F.2 Component Ablation on Phi-4-mini

The component ablation in Table 6 repeats the analysis of Section 5 on Phi-4-mini. The ranking of components reproduces the Qwen3-4B result: direction anchoring is the most critical, followed by state tracking, with clipping and the prior contributing modestly. The "remove anchoring" row falls below GRPO on AIME’24, reproducing the inversion-failure pattern documented in the main text.

F.3 Pass@K Results

Table 7 reports Pass@K for $K \in \{1, 4, 8, 16\}$ on MATH-500 and AIME’24, estimated from 32 samples per problem. OPPO improves Pass@K at every sampling budget on both benchmarks,

Table 5: Full results on Phi-4-mini (base). All methods are trained on DeepScaleR.

Method	GSM8K	M-500	AMC'23	AIME'24	GPQA-D	ARC-C	LCB
Base model	68.0	42.5	22.0	3.3	25.6	72.8	14.5
+ GRPO	76.8	55.2	35.0	8.3	29.4	78.6	19.2
+ Dr.GRPO	77.0	55.4	35.2	8.5	29.6	78.8	19.4
+ DAPO	78.2	57.0	37.5	10.0	30.4	79.4	20.2
+ SDPO	78.6	57.8	38.0	10.5	30.8	79.8	20.6
+ Self-OPPO	80.4	60.2	41.5	13.3	32.4	81.0	22.4
+ Teacher-OPPO	81.5	62.0	43.5	15.0	33.6	81.6	23.6
+ Dr.GRPO + OPPO	80.6	59.8	40.8	12.8	32.0	80.8	22.0
+ DAPO + OPPO	82.0	61.5	43.0	14.5	33.2	81.4	23.2

Table 6: Component ablation on Phi-4-mini. The ranking of components matches the Qwen3-4B result, with direction anchoring the most critical and state tracking second.

Configuration	M-500	AMC	AIME'24	GPQA
Self-OPPO (full)	60.2	41.5	13.3	32.4
remove anchoring	52.0	30.5	5.0	27.8
remove tracking	57.5	38.0	10.8	30.6
remove clipping	59.5	40.5	12.5	32.0
remove prior	59.8	41.0	13.0	32.2
log λ_t only	56.5	36.5	9.5	29.8
GRPO (uniform)	55.2	35.0	8.3	29.4

indicating that the gains over GRPO and SDPO are not driven by sharpening a single dominant mode at the expense of diversity. The relative improvement is largest at small K on AIME'24, where the base policy spreads probability across many incorrect reasoning paths and the Bayesian advantage redistributes credit toward the few that succeed.

Table 7: Pass@ K on Qwen3-4B. OPPO outperforms GRPO and SDPO at every sampling budget on both benchmarks.

Method	MATH-500				AIME'24			
	@1	@4	@8	@16	@1	@4	@8	@16
GRPO	72.6	82.0	86.5	90.2	26.7	40.0	48.3	56.7
SDPO	74.8	83.5	87.8	91.0	29.0	43.3	51.7	60.0
Self-OPPO	76.5	85.2	89.4	92.5	31.7	46.7	55.0	63.3
Teacher-OPPO	78.0	86.5	90.2	93.0	33.3	48.3	56.7	65.0

G Hyperparameter Sensitivity

We study the sensitivity of Self-OPPO on Qwen3-4B to the three method-specific hyperparameters: evidence clip bound C , Beta prior strength α , and group size G .

G.1 Evidence Clip Bound C

The clip bound C in Eq. (20) controls the per-token contribution to the running log-odds. Table 8 reports performance across five settings.

Setting C too small ($C = 1.0$) truncates genuine evidence at pivotal tokens, compressing the dynamic range of A_t toward the uniform-advantage regime. Setting C too large ($C = 10.0$) lets single tokens dominate the log-odds, saturating V_t prematurely and silencing later positions. Performance is stable across $C \in [2.0, 5.0]$, and the choice $C = 3.0$ used in the main experiments sits at the center of the stable region.

Table 8: Sensitivity to evidence clip bound C on Qwen3-4B.

C	1.0	2.0	3.0	5.0	10.0
MATH-500	74.8	76.0	76.5	76.2	75.5
AIME'24	29.0	31.0	31.7	31.3	30.0

G.2 Beta Prior Strength α

The Beta prior in Eq. (20) smooths the empirical group success rate before converting it to log-odds. Table 9 reports performance across five settings.

Table 9: Sensitivity to Beta prior strength α on Qwen3-4B.

α	0.1	0.5	1.0	2.0	5.0
MATH-500	76.0	76.3	76.5	76.4	75.8
AIME'24	30.8	31.3	31.7	31.5	30.5

Small α makes \hat{V}_0 responsive to the empirical success rate but produces extreme initial log-odds in all-correct or all-incorrect groups. Large α pulls \hat{V}_0 toward 0.5 regardless of the group composition and weakens the prompt-difficulty adaptation discussed in Section 3.3. Performance is stable across $\alpha \in [0.5, 2.0]$, and $\alpha = 1$ corresponds to a Laplace prior that is the standard choice for a Bernoulli outcome.

G.3 Group Size G

The group size G controls both the granularity of the prior $\hat{V}_0 = (k + \alpha)/(G + 2\alpha)$ and the variance of the GRPO sequence-level advantage that drives direction anchoring. Table 10 reports performance across four settings.

Table 10: Sensitivity to group size G on Qwen3-4B. OPPO improves over GRPO at every group size.

G	4	8	16	32
GRPO	70.8	72.6	73.5	74.0
Self-OPPO	74.5	76.5	77.2	77.5
Δ	+3.7	+3.9	+3.7	+3.5

Larger groups improve both GRPO and OPPO by reducing the variance of \hat{V}_0 . The improvement of OPPO over GRPO is stable across group sizes, indicating that the token-level credit assignment provides gains complementary to the group-based prior estimation rather than depending on a particular group size.

H Additional Analysis

H.1 Value Estimation Accuracy

The state-weight argument in Section 3.3 requires that intermediate V_t track the evolving success probability, not merely that the terminal V_{T+1} converge to R . We assess calibration on 500 MATH-500 trajectories from Qwen3-4B at four positions: $t = T/4, T/2, 3T/4, T$. Calibration at each position is measured by the Brier score

$$\text{BS}(t) = \frac{1}{N} \sum_{i=1}^N (V_t^{(i)} - R^{(i)})^2, \quad (40)$$

which equals 0 when the predicted success probability matches the empirical success rate at every decile.

Table 11: Brier score of V_t at four positions along the trajectory, on 500 MATH-500 trajectories. Lower is better.

Oracle estimator	$T/4$	$T/2$	$3T/4$	T
Self (4B)	0.071	0.058	0.049	0.042
Teacher (32B)	0.054	0.043	0.034	0.028

The Brier score decreases monotonically along the trajectory under both estimators, consistent with the recursion sharpening the posterior as more evidence is observed. The curves stay close to the diagonal at every position for both estimators, with the teacher curves consistently tighter in the mid-range $V_t \in [0.3, 0.7]$ where the state weight $V_t(1 - V_t)$ has the largest effect on the gradient. The intermediate calibration confirms that $V_t \approx \frac{1}{2}$ corresponds to roughly 50% empirical success, so the state-weight modulation peaks where the outcome is genuinely uncertain rather than at an artefact of the recursion.

H.2 Computational Overhead

OPPO requires one additional forward pass per trajectory for oracle evaluation. Table 12 reports wall-clock training time per step on $2 \times$ H200 GPUs.

Table 12: Wall-clock time per training step on $2 \times$ H200 GPUs.

Method	Forward passes	Time/step (s)	Overhead vs. GRPO
GRPO	1 (rollout) + 1 (policy)	12.4	—
Self-OPPO	1 (rollout) + 1 (oracle) + 1 (policy)	16.8	+35%
Teacher-OPPO	1 (rollout) + 1 (oracle, 32B) + 1 (policy)	24.2	+95%

The self-oracle overhead is moderate (+35%) because the oracle forward pass uses the same model as the policy and can share the KV cache from the standard forward pass. The teacher-oracle overhead is larger (+95%) because the 32B estimator runs on separate weights, but the cost can be amortized by batching oracle evaluations across trajectories within a step and by offloading the estimator to dedicated devices when available.

I Implementation Details

I.1 Training Configuration

All experiments use the verl framework [30] on $2 \times$ H200 GPUs with the configuration in Table 13.

I.2 Oracle Prompt Format

For self-oracle evaluation, the ground-truth answer y^* is appended to the prompt before the model’s response, in the format

```
[Standard prompt]
Question: {question}
[Oracle augmentation]
The answer is {y*}.
[Model response]
{y_1, y_2, ..., y_T}
```

The oracle-conditioned forward pass scores the same response tokens $y_{1:T}$ under the augmented prompt, while the standard forward pass scores them under the original prompt. The log-likelihood ratio $\log \lambda_t$ is the per-token difference between the two scores. No generation is performed during oracle evaluation, so the cost reduces to two forward passes per trajectory rather than two decoding runs.

Table 13: Training hyperparameters used for all main-text experiments.

Hyperparameter	Value
Optimizer	AdamW
Learning rate	1×10^{-6}
Weight decay	0.01
Warmup steps	10
Learning-rate schedule	cosine decay
Global batch size	32
Group size G	8
Maximum response length	8192 tokens
Maximum prompt length	1024 tokens
Sampling temperature	1.0
PPO clip ϵ	0.2
Evidence clip C	3.0
Beta prior α	1
Training epochs	1
Gradient checkpointing	enabled
Precision	bfloat16

I.3 Reward Function

We use exact-match reward: $R = 1$ if the extracted numerical answer matches the ground-truth integer and $R = 0$ otherwise. Answer extraction follows the standard boxed-answer format used in DeepScaleR. No partial-credit or format-bonus rewards are used, so the binary outcome reward is the only environment signal driving direction anchoring.